

THEORETICAL AND NUMERICAL ANALYSES OF STEEL-TIMBER COMPOSITE BEAMS WITH LVL SLABS

Julia STRZELECKA, Łukasz POLUS¹, Marcin CHYBIŃSKI
Institute of Building Engineering, Faculty of Civil and Transport Engineering,
Poznan University of Technology, Poland

Abstract

Recently conducted studies have shown that significant benefits are to be gained by joining steel beams and timber slabs. Steel-timber composite beams present a sustainable solution for the construction industry because of their high strength and stiffness, and lower carbon footprint and self-weight than steel-concrete composite beams. The behaviour of steel-timber composite beams is still being investigated to reduce knowledge gaps. This paper presents theoretical and numerical analyses of steel-timber composite beams consisting of steel girders and laminated veneer lumber slabs. The elastic and plastic resistance to bending were estimated analytically based on the elastic analysis and the rigid-plastic theory. The impact of the composite action, the LVL slab thickness, the cross-section of a steel girder and the steel grade on resistance to bending was evaluated. The load-deflection curve of the composite beam was obtained using a 2D finite element model, in which timber failure was captured using the Hashin damage model. The results of the numerical simulation were in good agreement with the ones of the theoretical analyses.

Keywords: steel-timber composite beams, laminated veneer lumber (LVL), finite element method (FEM)

1. INTRODUCTION

Sustainable construction is an important trend in civil engineering. New solutions using renewable, green building materials with a low embodied carbon footprint are preferred [1]. Buildings with timber structural elements store carbon for decades and reduce dependence on non-renewable materials [2]. For this reason, timber – one of the oldest building materials – is still used in structures. Thanks to engineering wood products such as laminated veneer lumber (LVL), new applications for timber are developed. The benefits of engineering wood products include decreased impact of imperfections, more homogenous mechanical properties, increased dimensional stability, greater durability and development of bigger structural elements [3, 4]. LVL consists of several glued softwood veneers about 3 mm thick [5]. In Poland, LVL is made from pine and spruce [6]. Defects in LVL are evenly distributed because

¹ Corresponding author: Institute of Building Engineering, Faculty of Civil and Transport Engineering, Poznan University of Technology, Piotrowo 5 Street, 60-965 Poznan, Poland, lukasz.polus@put.poznan.pl, +48-61-665-2098

knots are limited to a single sheet of veneer [7]. In the case of LVL production, wood resources are used efficiently. LVL slabs and beams can be obtained from trees of relatively small diameters thanks to using the rotary peeling method. LVL beams can be easily and quickly reinforced with carbon fibre-reinforced polymer sheets [8]. LVL is used in floor structures, roof diaphragms and overhangs, lintels, building walls and I-beam flanges [6, 9–12]. One of the relatively new applications for LVL are steel-timber composite beams. Steel and timber can be used effectively in structural elements. Steel connectors have long been used to join timber elements. However, not only steel connectors can be used with timber. Ganowicz and Plenzler used 6 and 8 mm steel bars in their tests to reinforce the tensioned parts of the timber beams [13, 14]. Based on the results of these tests, in 1977, timber purlins reinforced with steel bars were used in a hall roof in Poznań. Jasińko used epoxy resin, steel plates and bars to reinforce timber beams [15–18] (Fig. 1). Rapp elaborated and used in practice adhesive finger timber joints reinforced with steel plates [19].

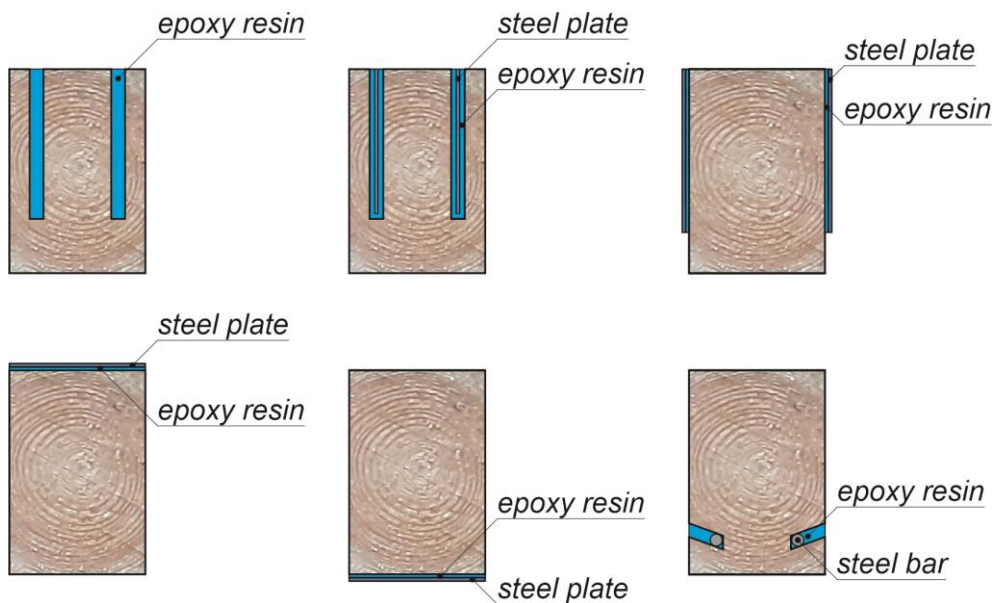


Fig. 1. Timber reinforced beams tested by Jasińko [15–18]

In the above solutions steel elements were only used as reinforcement of timber beams. However, steel and timber can also be used in a single composite member. A composite structural beam is composed of minimum two parts. The parts are made of materials of different properties and they are permanently connected [20]. The components are connected using shear connections, which play a crucial role and transfer the longitudinal shear force in composite beams [21]. Thanks this combination, multiple benefits can be gained, e.g., reduced weight, better material efficiency [22]. Composite beams have a higher load-bearing capacity and stiffness than non-composite elements [23]. For this reasons, it is possible to reduce deflections and use a lower cross-section [24]. Furthermore, slabs increase the local and lateral stability of the girders [25]. In 1984, the project of a steel-wood composite bridge was demonstrated at the 12th IABSE Congress in Canada [26]. The bridge was completed in 1993 and the results of its field tests were presented by Bakht and Krisciunas [27]. It consisted of a post-tensioned laminated wood deck, welded plate steel girders and steel cross-frames. The composite action was achieved through the shear bulkheads, i.e., shear studs installed on the girder flanges and located in large holes drilled in the slab and filled with expansive concrete (Fig. 2).

Steel-timber composite structures have several important performance characteristics which make them sustainable: small self-weight, high strength to weight ratio, fast assembly, low environmental impact, and possibility of demounting and recycling elements at the end of their service life. Full-dry systems make it possible to speed up the assembly process of such structures. The use of timber results in reduced carbon footprint. LVL ($8 \times 10^{-6} \text{ 1/}^\circ\text{C}$ [28]) and steel ($12 \times 10^{-6} \text{ 1/}^\circ\text{C}$ [29]) have similar thermal expansion coefficients; therefore, temperature change will not cause stress at the interlayer. Timber slabs have a lower self-weight than slabs made of concrete used in steel-concrete composite beams. For this reason, the use of timber reduces not only the dead load of the structure, but also seismic forces.

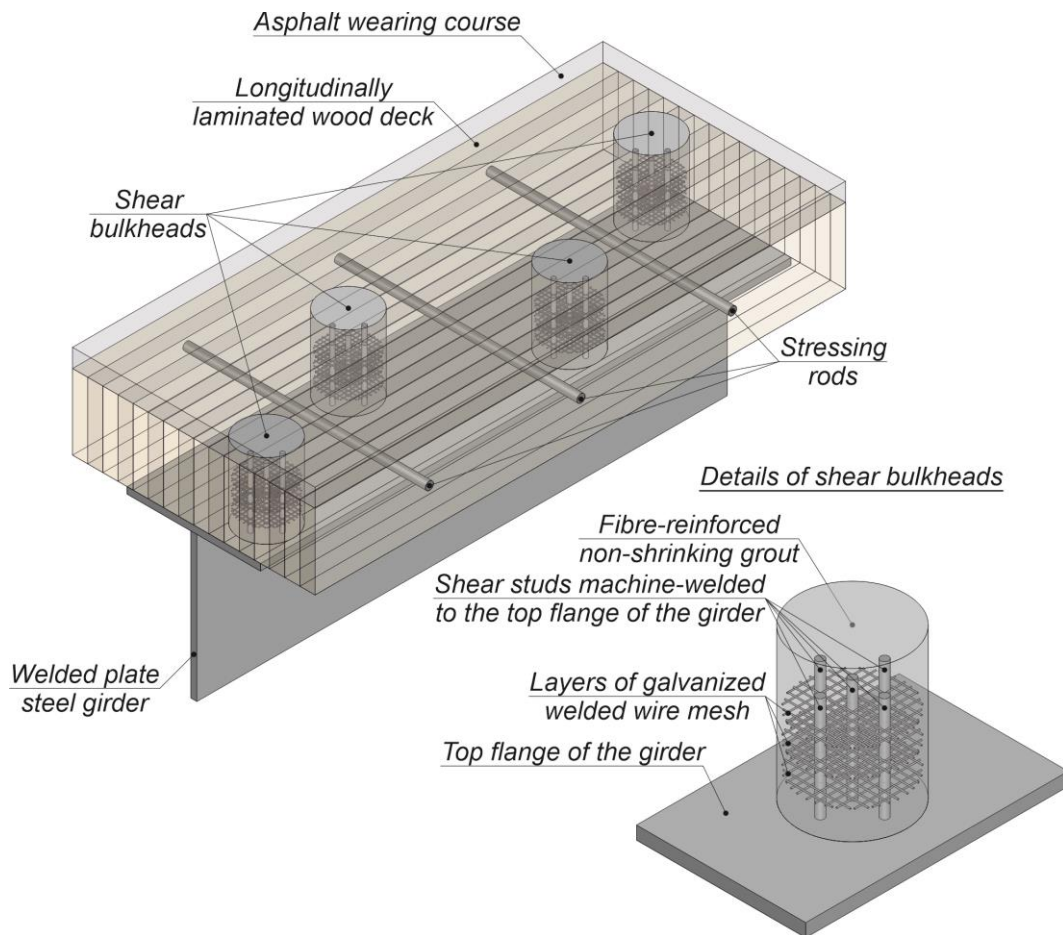


Fig. 2. Shear connections used in the first steel-timber composite bridge [27]

However, there are some disadvantages to using steel-timber composite structures. The first one is the low fire resistance of steel-timber composite elements. This, however, can be remediated by using fire protective materials [30]. Steel girders can be encased by timber elements [31]. Alternatively, fire resistance can be improved by using stainless steel, which loses strength at fire slower than carbon steel [32]. Despite the fact that many analyses have been conducted on steel and timber composite structures, no standards for designing such structures have been developed. However, in 2022, Design Guide 37 was published, and it contained a multi-disciplinary review of hybrid steel-timber structures [33]. Another disadvantage of steel-timber structures results from the fact that corrosion of steel girders can cause structural failure. For this reason, steel girders should be protected against it. Stainless steel or

aluminium alloys may also be used instead of carbon steel [34, 35]. The use of stainless steel can provide for a durable solution. Stainless steel is more expensive than carbon steel but has low maintenance costs. What is more, stainless steel exhibits superior stiffness and strength retention at high temperatures and greater thermal expansion than carbon steel [36–38]. Last but not the least, it is impossible to achieve full shear interaction, since connections used in steel-timber structures are flexible and slip occurs at the interface [39]. However, it is possible to obtain a steel-timber beam with full shear connection, in which the number of the shear connectors is such that the load-bearing capacity of the beam is controlled by the flexural capacity of the steel-timber composite beam, and not by the shear capacity of the connections. Steel-timber composite beams have many applications. They can be used in prefabricated buildings, bridges and footbridges. They can also be used in multi-story buildings at seismic areas due to their light weight, which reduces the seismic forces [40, 41]. Furthermore, they can be applied in rehabilitation work. Existing timber ceilings and bridges can be reinforced with steel structural elements. Both beams and columns can be developed as steel-timber composite elements. A sustainable steel-timber composite beam consists of a steel girder and a timber panel. Steel girders in steel-timber composite beams can be made of hot-rolled, welded or cold-formed steel beams (Fig. 3).

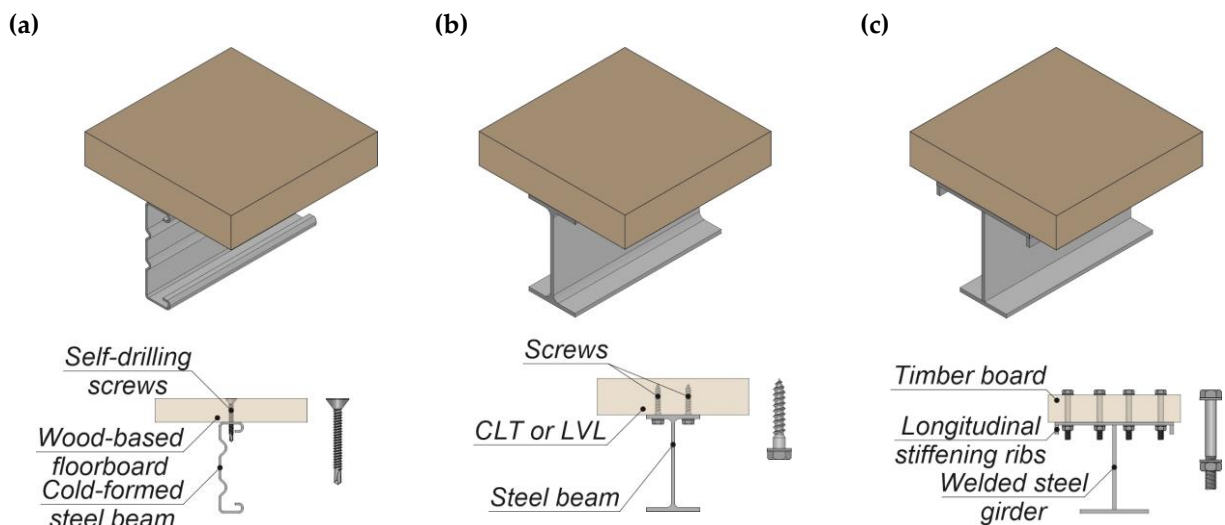


Fig. 3. Steel-timber composite beams with: (a) a cold-formed girder [42]; (b) a hot-rolled girder [43]; (c) a welded girder [44]

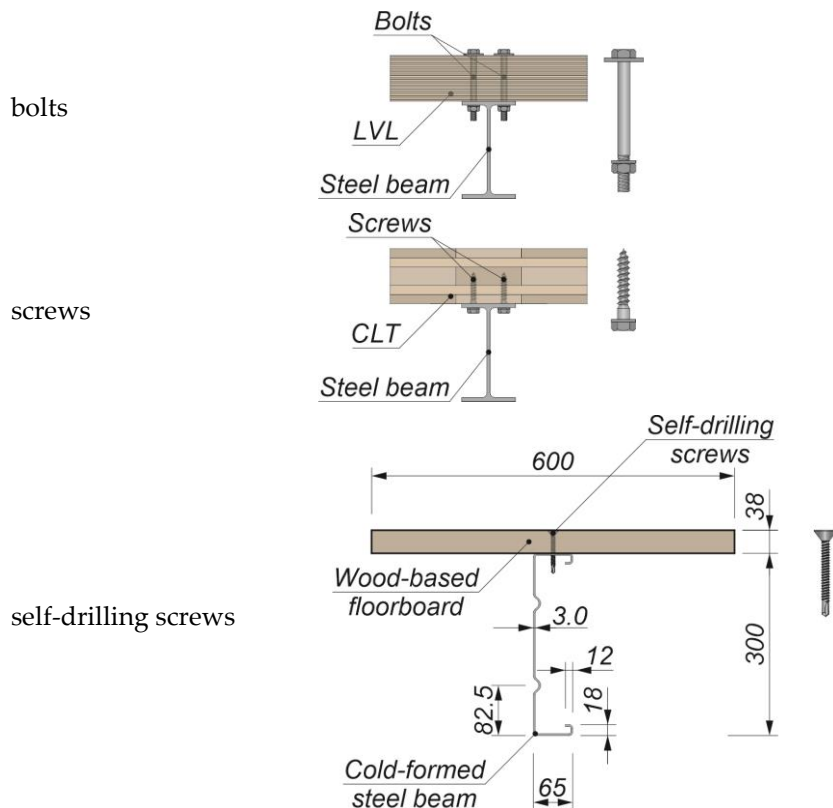
The use of thin-walled steel structures reduces steel consumption [45]. Cold-formed steel beams are light, which results in lower transportation costs and faster construction of buildings. However, thin-walled structures are at risk of buckling and when they are designed, stability problems should be taken into account [46]. It is possible to improve the structural performance and the load-carrying capacity of cold-formed steel elements by combining them with the structural elements made of timber. Derlatka developed a steel-oriented strand board composite beam consisting of steel thin walled plates and oriented strand boards [47]. Awaludin et al. attached timber laminated elements to the webs of cold-formed steel beams using screws (Fig. 4) [48]. Composite steel-timber and reference steel beams were subjected to compression tests. Elements of five different lengths were analysed, i.e., 200 mm, 300 mm, 600 mm, 900 mm, and 1200 mm. The load-carrying capacity of the cold-formed steel beams increased

1.4–6.7 times after they had been joined with timber elements. The lowest increase in the load-bearing capacity was observed in the longest elements.



Fig. 4. Composite steel-timber elements tested by Awaludin et al. [48]

Attaching timber elements to the webs of cold-formed steel beams is not the only possible solution. Wood-based particle boards were connected with cold-formed steel joists by Kyvelou et al. The results of numerical tests showed that the flexural capacity of the analysed composite element increased by 140% and its stiffness increased by 40% [42]. Timber slabs can be made of cross laminated timber (CLT), laminated veneer lumber (LVL) or wood-based particle boards. There are several types of shear connectors used in steel-timber composite structures, i.e., screws, bolts, screws with epoxy adhesive, bolts embedded in grout, bolt-in-tube connections, screws surrounded by outer fittings (Fig. 5) [49–57].



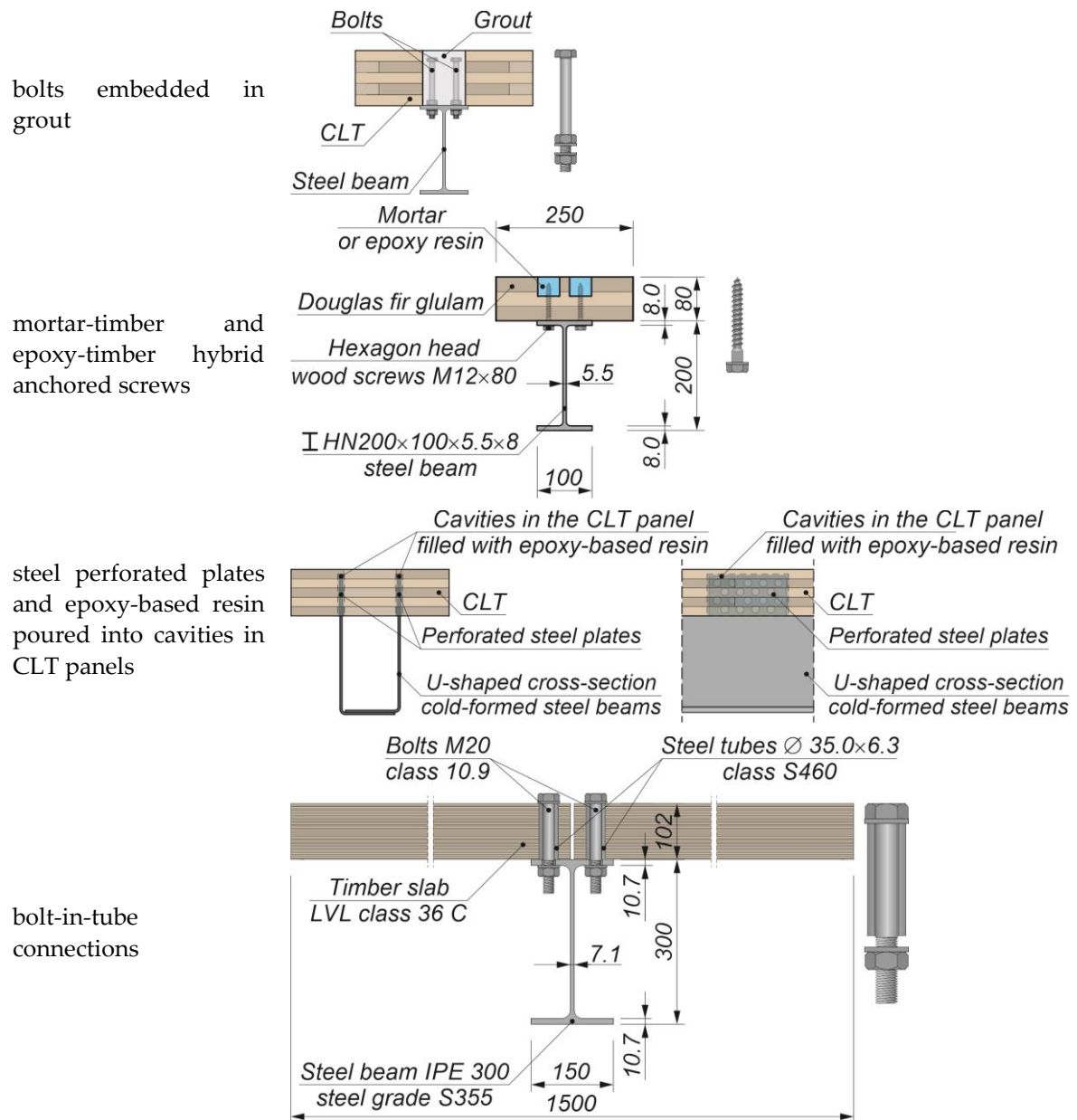


Fig. 5. Shear connections used in steel-timber composite beams [50–57]

The recently conducted studies have not eliminated all knowledge gaps. Design provisions are still lacking [58]. New and innovative solutions require a significant amount of research to demonstrate that all requirements for construction industry can be met [59]. For this reason, the behaviour of sustainable steel-timber composite elements is still being investigated. In this paper, the results of theoretical analyses and a numerical simulation of a steel-timber composite beam were compared. Based on the theoretical and numerical analyses, the increase in the load-carrying capacity and stiffness of a steel girder after connecting it with an LVL slab were evaluated. The numerical model can be used in future numerical analyses, such as parametric studies.

2. THEORETICAL ANALYSES

2.1. Theoretical models

The theoretical analyses were based on a few assumptions. It was assumed that the beams acted as monolithic beams (full shear interaction). This assumption is difficult to achieve in regular beams because the longitudinal slip between the beam components cannot be completely eliminated, since connectors always undergo deformation. However, the slip can be reduced by using an epoxy adhesive in connections and a higher number of connectors [43]. Secondly, it was assumed that the analysed steel-timber beams were with full shear connections. It means that the number of the employed connectors was such that the load-bearing capacity of the beams was controlled by the flexural capacity of the steel-timber beams and not by the shear capacity of their connections. Yet another assumption referred to timber. The timber subjected to tension in the slab was taken into account in the flexural capacity calculations. In the case of steel-concrete composite beams, the concrete subjected to tension was not taken into account [60]. The LVL tension strength (parallel to grain) was only 1.11 times lower than the LVL compression strength (parallel to grain) [6]. For this reason, the impact of the timber subjected to tension on the flexural capacity was taken into account. In the calculations of the plastic resistance moment of the composite cross-sections, the effective area of the LVL in compression resisted a stress equal to the LVL compression strength (parallel to grain), constant over the whole depth between the plastic neutral axis and the most compressed fibre of the LVL. The effective area of the LVL in tension resisted a stress equal to the LVL tension strength (parallel to grain), constant over the whole depth between the plastic neutral axis and the most tensioned fibre of the LVL. The models used to calculate the elastic and the plastic resistance to bending of the steel-timber composite beams are presented in Figs. 6 and 7.

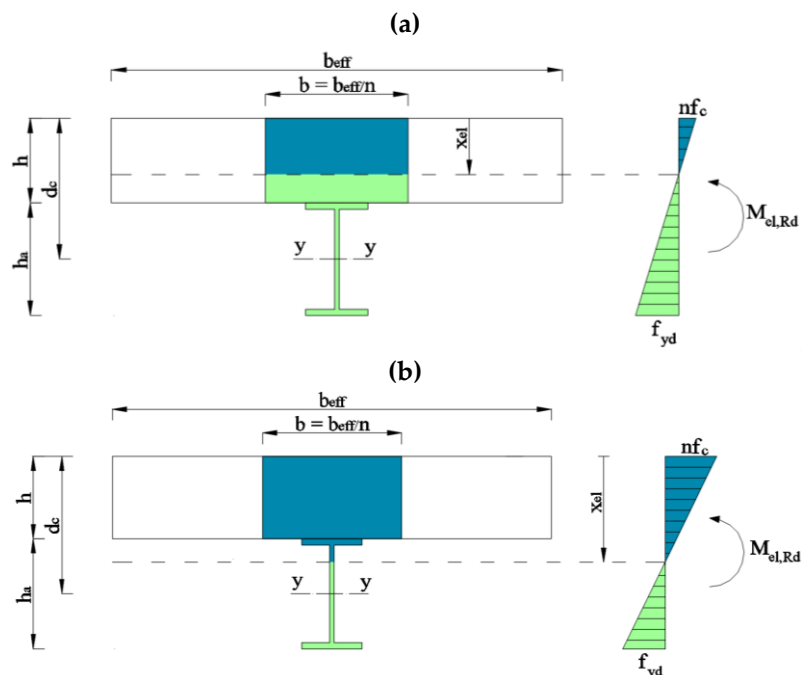


Fig. 6. The model used to calculate the elastic resistance to bending of the steel-timber composite beams: (a) the elastic neutral axis is in the timber slab; (b) the elastic neutral axis lies within the steel section

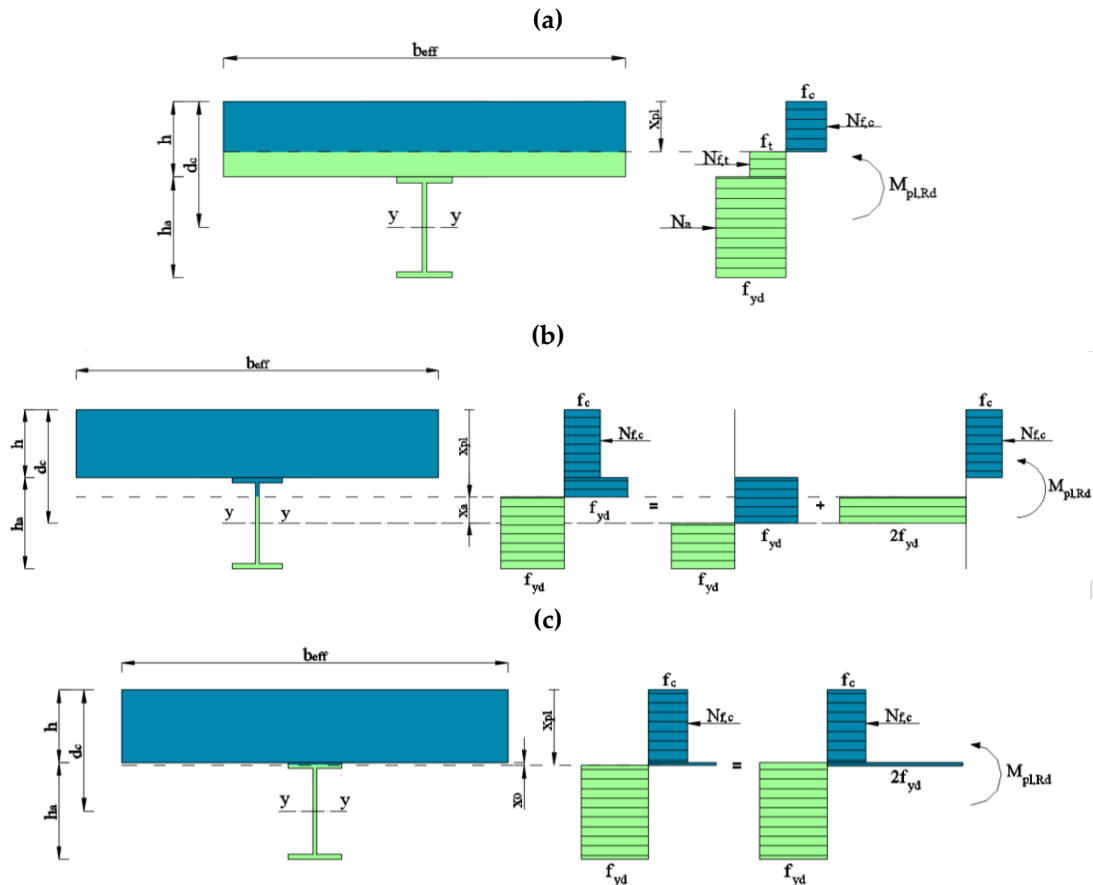


Fig. 7. The model used to calculate the plastic resistance to bending of the steel-timber composite beams: (a) the plastic neutral axis is in the timber slab; (b) the plastic neutral axis lies within the web of the steel beam; (c) the plastic neutral axis lies within the flange of the steel beam

2.2. The impact of composite action on resistance to bending

A 4-metre simple supported girder (IPE 100) made of S235 steel was connected with an LVL slab to evaluate the impact of composite action [61]. The effective width of the slab was 1000 mm and its thickness was 75 mm. The design lateral torsional buckling resistance moment of a laterally unrestrained girder $M_{b,Rd}$ was 4.27 kNm. The moment capacity of the bare steel section $M_{c,Rd}$ was 9.26 kNm. The design elastic and plastic resistance to bending of the steel-timber composite beam are presented in Tables 1 and 2.

Table 1. The design elastic resistance to bending of the steel-timber composite beam

Parameter	Value
Modular ratio n [–]	15.0
Ideal slab width b [mm]	66.7
Location of the neutral axis x_{el} [mm]	48.6
Second moment of area I_y [cm ⁴]	1068.2
Design compressive strength of LVL (parallel to grain) f_{cd} [MPa]	26.7
Design yield strength of steel f_{yd} [MPa]	235.0
Design elastic bending resistance $M_{c,el,Rd}$ [kNm]	19.86

Table 2. The design plastic resistance to bending of the steel-timber composite beam

Parameter	Value
Location of the plastic axis x_{pl} [mm]	40.3
Design tensile strength of LVL (parallel to grain) f_{td} [MPa]	24.0
Design plastic bending resistance $M_{c,pl,Rd}$ [kNm]	56.61

The design plastic moment resistance of the beam section increased from 9.26 kNm to 56.61 kNm (6.1 times) after the steel girder was connected with the LVL slab (Fig. 8). In the case of the laterally unrestrained steel girder, the increase in the load-bearing capacity was higher because the cooperation of the steel girder with the LVL slab eliminates the problem of lateral-torsional buckling in simply supported beams. The load-bearing capacity of the laterally unrestrained steel girder increased from 4.27 kNm to 56.61 kNm.

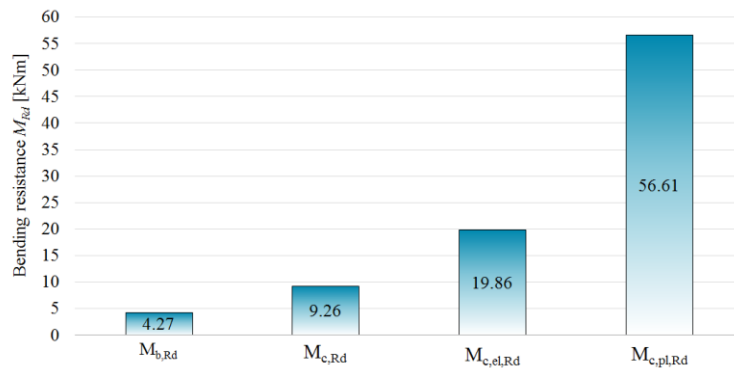


Fig. 8. The design resistance to bending of the steel girder and the steel-timber composite beam

2.3. The impact of LVL slab thickness on resistance to bending

The increase in the LVL slab thickness provided for the increase in the bending resistance (Fig. 9).

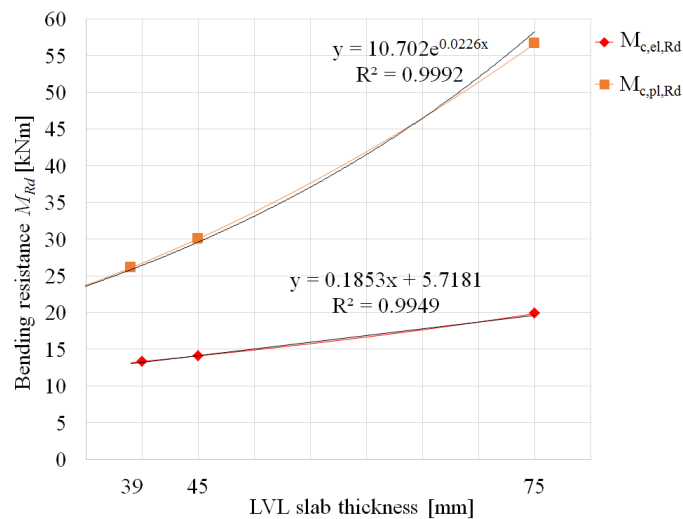


Fig. 9. The impact of the LVL slab thickness on the design resistance to bending of the steel-timber composite beam

In the case of elastic bending resistance, the increase was linear, whereas in the case of plastic bending resistance, exponential growth was observed. The markers represent the results for the analysed LVL slab thickness [6].

2.4. The impact of the steel girder cross-section

Using a larger cross-section provided for the increase in the bending resistance (Fig. 10). In the case of elastic bending resistance, the bending resistance growth was linear, whereas in the case of plastic bending resistance, it was exponential. The markers represent the IPE cross-sections.

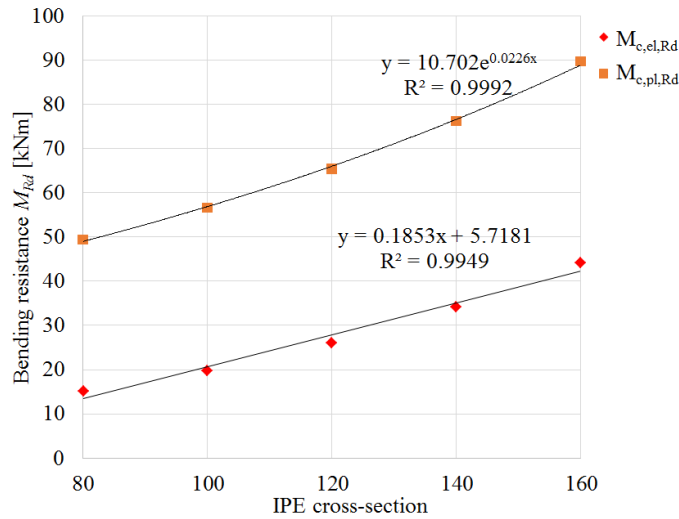


Fig. 10. The impact of the steel girder cross-section on the design resistance to bending of the steel-timber composite beam

2.5. The impact of the steel grade

The steel grade had an impact on the bending resistance (Fig. 11).

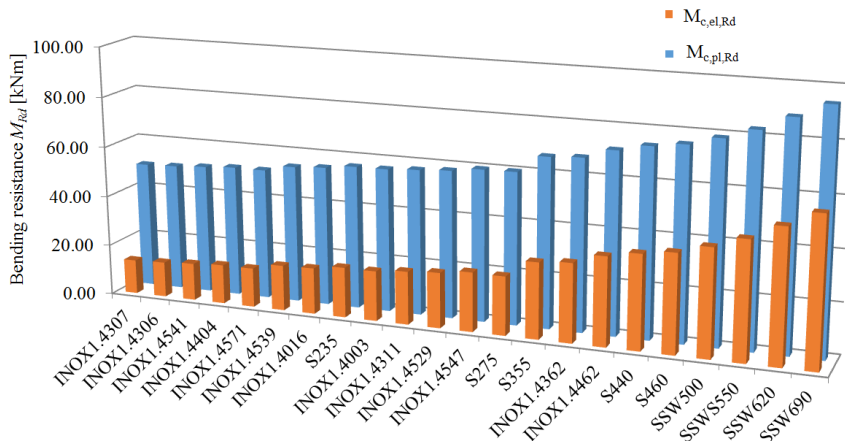


Fig. 11. The impact of the steel grade on the design resistance to bending of the steel-timber composite beam with an IPE 100 girder

The increase in the yield strength of the steel provided for the increase in the bending resistance. The changing of both the cross-section and the steel grade had a strong impact on the plastic bending resistance of the steel-timber composite beam (Fig. 12).

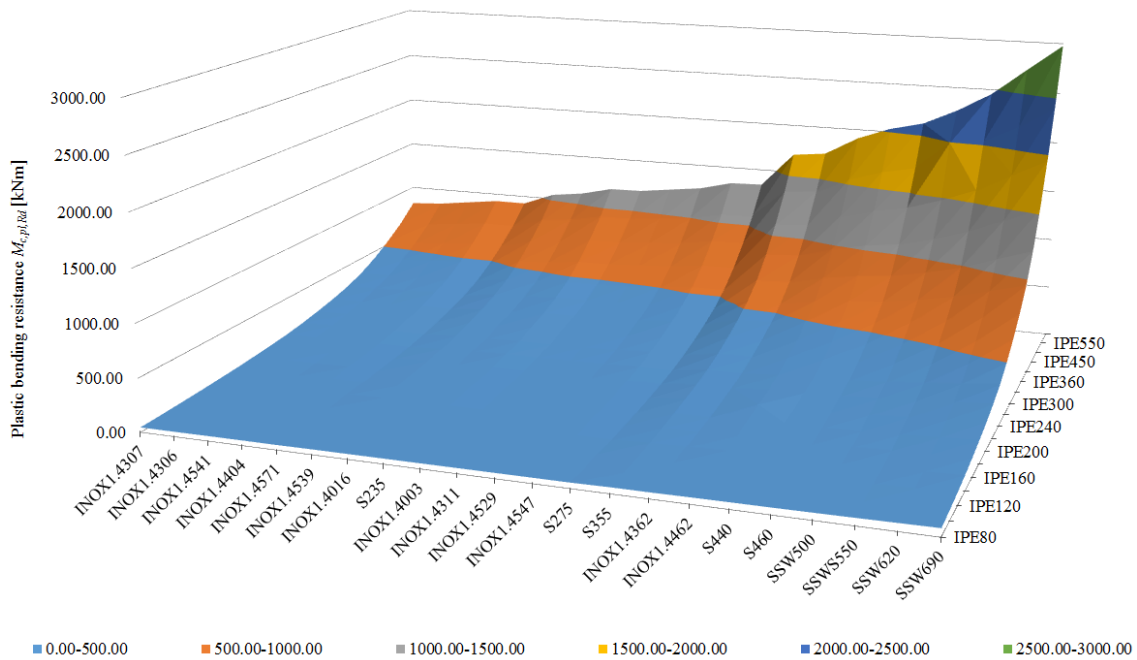


Fig. 12. The impact of the steel girder cross-section and the steel grade on the design resistance to bending of the steel-timber composite beam

2.6. Worked example

The authors analysed two steel-timber composite beams differing in girder material. Each beam was 2.7 m long and consisted of a steel girder (IPE 140) and an LVL slab (75 mm × 370 mm). In the first beam, the girder was made of S355 steel, whereas in the second it was made of 1.4547 stainless steel. The characteristic yield strength of 1.4547 stainless steel (300 MPa) is comparable to that of S355 steel (355 MPa). 1.4547 stainless steel is more expensive than S355 steel. However, it provides for low maintenance costs and increases durability. Furthermore, austenitic stainless steel exhibits higher strength at high temperatures (> 550°C) than carbon steel [62]. The elastic and the plastic resistance to bending of the steel-timber composite beams was calculated (Figs. 13 and 14, Tables 3 and 4). In these analyses, the characteristic parameters of the materials were used. The results of the analysis of the composite beam with the S355 girder were later compared with the results of the numerical simulation presented in Chapter 3.

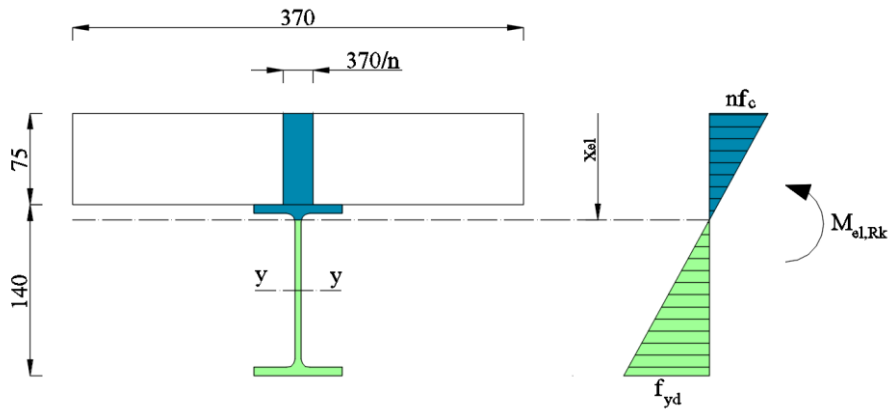


Fig. 13. The model used to calculate the elastic resistance to bending of the steel-timber composite beams

Table 3. The characteristic elastic resistance to bending of the steel-timber composite beams

Parameter	S355	1.4547
Modular ratio n [-]	15.0	13.9
Ideal slab width b [mm]	24.7	26.6
Location of the neutral axis x_{el} [mm]	87.5	85.6
Second moment of area I_y [cm ⁴]	1632.5	1674.0
Characteristic compressive strength of LVL (parallel to grain) f_{ck} [MPa]	40.0	40.0
Characteristic yield strength of steel f_{yk} [MPa]	355.0	300
Characteristic elastic bending resistance $M_{c,el,Rk}$ [kNm]	45.4	38.8

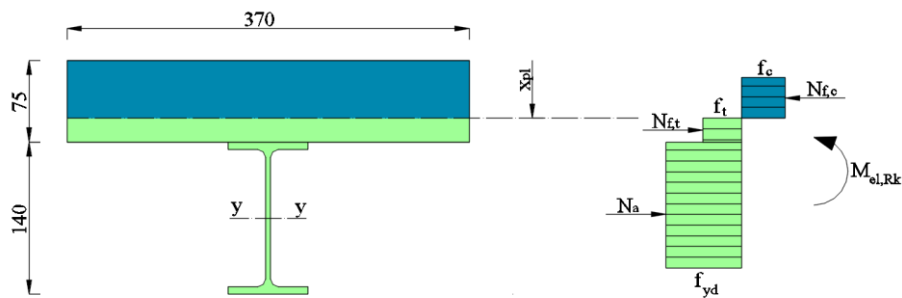


Fig. 14. The model used to calculate the plastic resistance to bending of the steel-timber composite beams

Table 4. The characteristic plastic resistance to bending of the steel-timber composite beams

Parameter	S355	1.4547
Location of the plastic axis x_{pl} [mm]	56.2	53.0
Characteristic tensile strength of LVL (parallel to grain) f_{tk} [MPa]	36.0	36.0
Characteristic plastic bending resistance $M_{c,pl,Rk}$ [kNm]	77.4	69.3

3. NUMERICAL ANALYSIS

3.1. Numerical model

The Abaqus program, which has been widely used for the analysis of composite beams [63–66], was chosen for the conducted numerical analysis. A 2D numerical model of the steel-timber composite beam consisted of a steel beam with stiffeners, an LVL slab, steel loading and support plates (Fig. 15). A four-point bending test was simulated (Fig. 16).

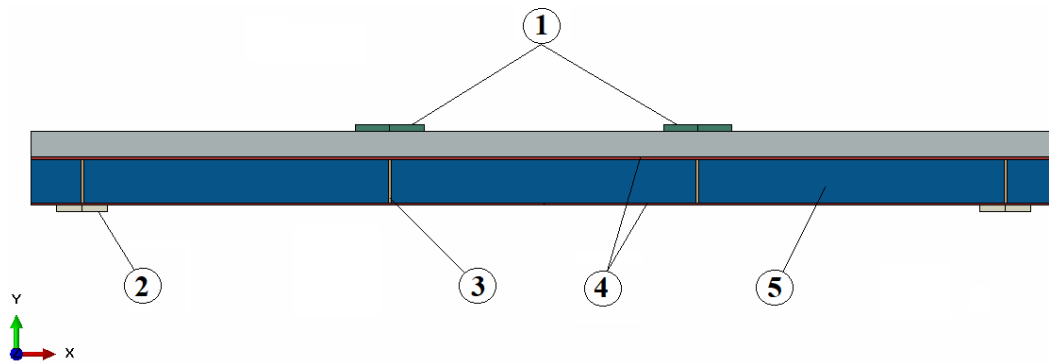


Fig. 15. The numerical model of the steel-timber composite beam: 1 – loading steel plates located on the LVL slab, 2 – support plate, 3 – stiffener, 4 – girder flanges, 5 – girder web

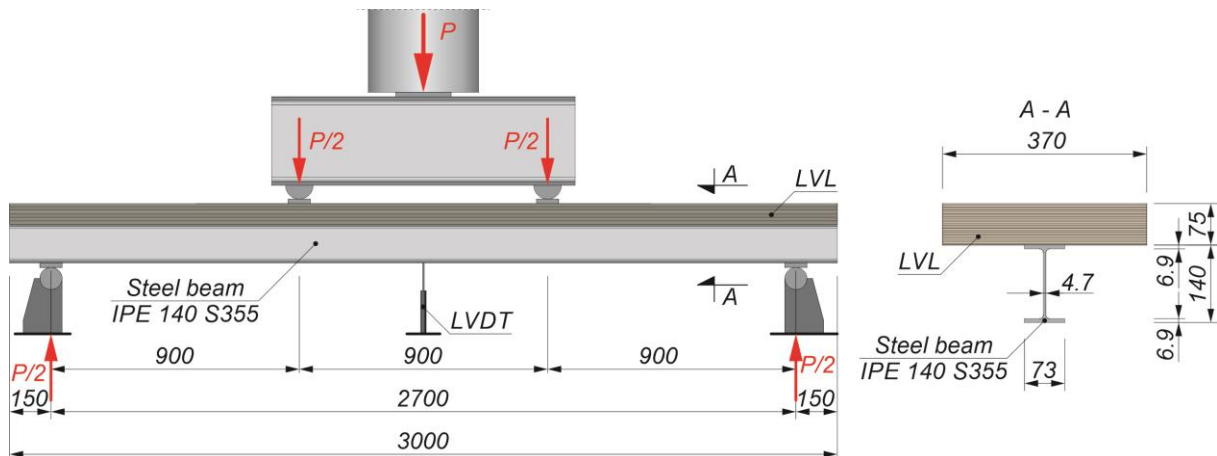


Fig. 16. The composite beam in the four point bending test

The behaviour of numerical models of composite beams depends, among others, on shear connection modelling and material characteristics. In this study, it was assumed that the analysed beam was a full composite beam. Full composite action was modelled by tying the contact surface between the girder flange and the LVL slab. The continuous “tie” type contact can be used to model full composite action [67]. The numerical analysis used the same assumptions as the theoretical analyses. However, full shear interaction is difficult to achieve because connections for steel-timber composite beams are flexible. For this reason, future studies should focus on the impact of the slip between the steel girder and the LVL

panel on the ultimate load and stiffness of steel-timber composite beams. The steel was described as a linear hardening material ($f_y = 235$ MPa, $E = 210$ GPa, $f_u = 490$ MPa). The LVL was modelled as an orthotropic material with a failure model. The Hashin damage model was used to capture the failure of LVL. The material parameters were based on the material tests and the numerical simulations of the LVL slabs [5] (Table 5). 4-node bilinear plane stress quadrilateral elements with reduced integration and hourglass control (CPS4R) were used to model all members. The maximum mesh size was 10 mm and the total number of finite elements was 7057 (Fig. 17).

Table 5. The properties of the LVL modelled as an orthotropic material with the Hashin damage model, based on [5] (1 – parallel to the laminated veneer lumber grain)

Elastic orthotropic material (lamina)					
E_1	E_2	ν_{12}	G_{12}	G_{13}	G_{23}
[MPa]	[MPa]	[-]	[MPa]	[MPa]	[MPa]
16 000	430	0.48	600	600	96
Hashin damage model					
σ_{t1}	σ_{c1}	σ_{t2}	σ_{c2}	σ_{v12}	σ_{v23}
[MPa]	[MPa]	[MPa]	[MPa]	[MPa]	[MPa]
41.9	50.3	10	15	10	5
Longitudinal tensile fracture energy [kJ/m ²]	Longitudinal compressive fracture energy [kJ/m ²]	Transverse tensile fracture energy [kJ/m ²]	Transverse compressive fracture energy [kJ/m ²]	Viscosity coefficient	
45	45	0.1	0.1	1.0×10^{-6}	



Fig. 17. The mesh used in the numerical simulation

The chosen point for the measurement of the deflection, the boundary conditions and the points where the displacement in y direction was set are presented in Fig. 18. The calculations were done using the Newton-Raphson method. Surface-to-surface “hard” contact and friction were defined between the steel plates and the LVL slab, and between the support plates and the steel beam. The friction coefficient was assumed as 0.3 [68]. The stiffeners were tied to the girder web and flanges and the flanges were tied to the girder web.

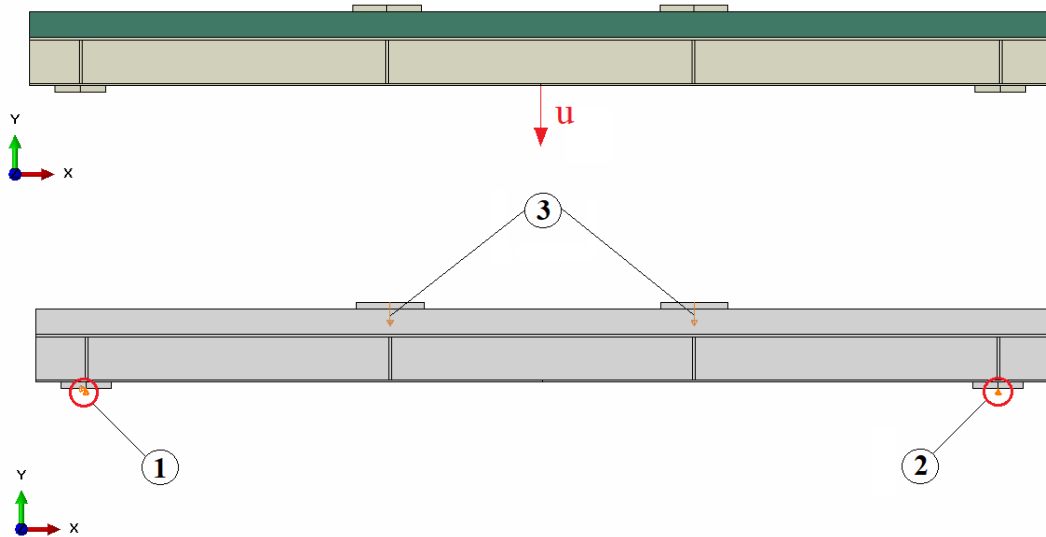


Fig. 18. The measure point and the boundary conditions: 1 – displacement in x and y directions (fixed), 2 – displacement in y direction (fixed), 3 – displacement in y direction

3.2. Results of the numerical analysis

Figure 19 summarises the results of the finite element analysis and presents a comparison between the values of resistance to bending of the steel-timber beam obtained in the theoretical and numerical investigations. In Figure 19, $M-u$ (FEA) represents the moment versus deflection curve from the numerical simulation, $M_{el,Rk,T}$ stands for theoretical elastic bending resistance, $M_{pl,Rk,T}$ stands for theoretical plastic bending resistance, and $M_{c,Rk,T}$ represents the flexural capacity of the bare steel section.

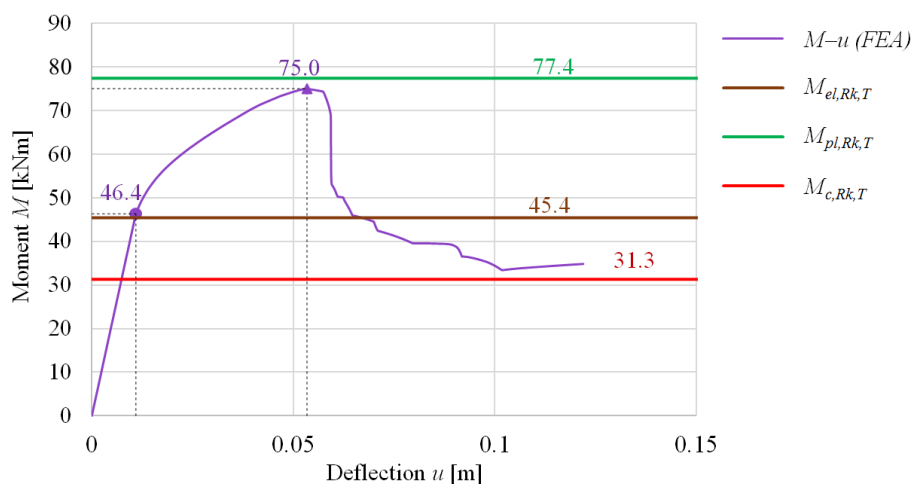


Fig. 19. The moment versus deflection from the numerical simulation and the comparison between the values of resistance to bending of the steel-timber beam obtained in the theoretical and numerical investigations

The elastic bending resistance was obtained in the numerical model when the steel achieved its yield strength at the bottom girder flange (Fig. 20).

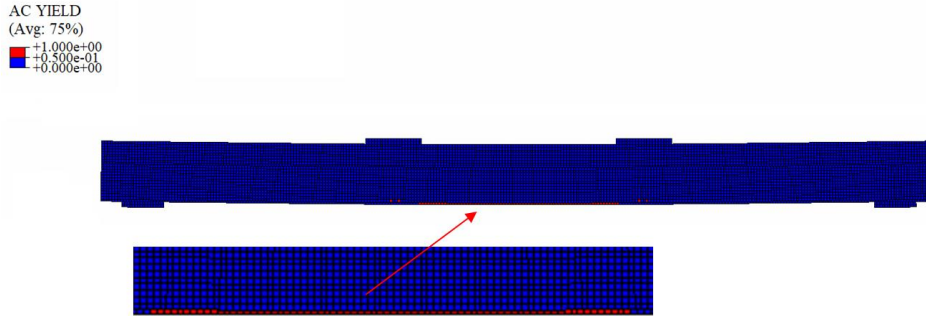


Fig. 20. The yield strength achieved at the bottom girder flange ($M = 46.4$ kNm)

The elastic bending resistance from the theoretical analysis (45.4 kNm) was 2.2% lower than the one from the numerical calculation (46.4 kNm). The load-bearing capacity of the steel-timber beam in the numerical analysis was achieved when a peak on the moment-deflection curve was observed. The plastic bending resistance from the theoretical analysis (77.4 kNm) was 3.1% higher than the one from the numerical calculation (75.0 kNm). The plastic moment resistance of the beam section increased 2.4 times after the steel girder was connected with the LVL slab. Due to the fact that the Hashin damage model was used in the numerical analysis, it was possible to observe the damage initiation in the LVL panel. HSNFCCRT is the fibre compressive initiation criterion and HSNFTCRT is the fibre tensile initiation criterion (Fig. 21) [69, 70]. At the ultimate moment ($M = 75.0$ kNm), the yield strength was achieved in the whole cross-section of the steel girder (Fig. 22).

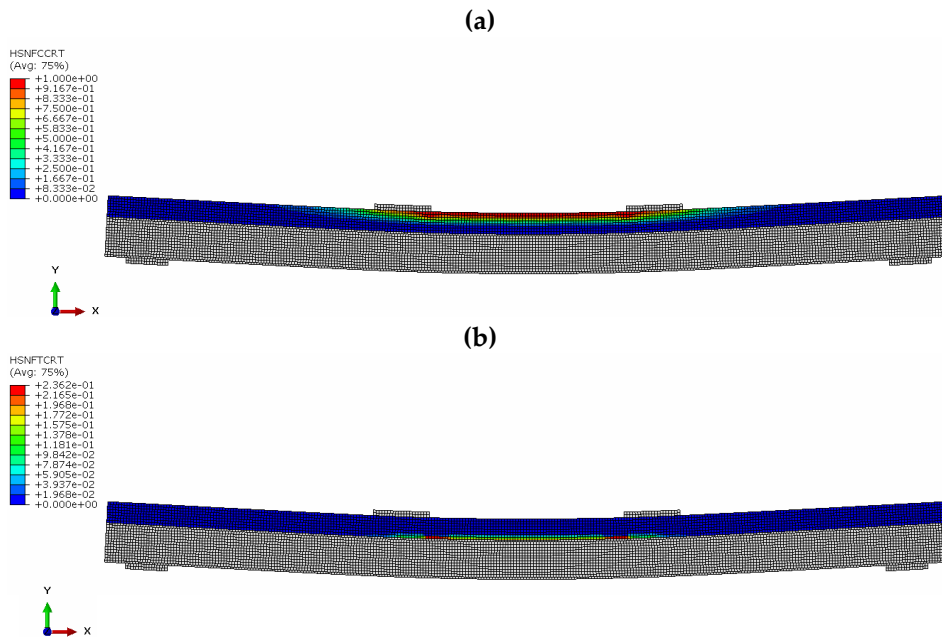


Fig. 21. Damage initiation areas: (a) due to the compression ($M = 75.0$ kNm); (b) due to the tension ($M = 75.0$ kNm)

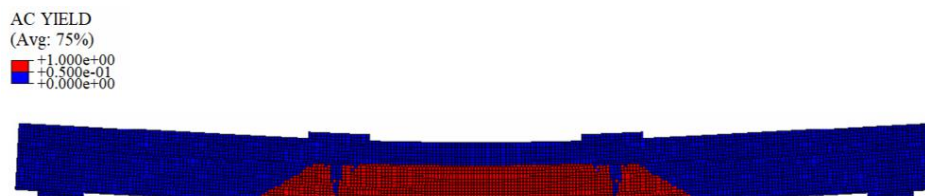


Fig. 22. The yield strength achieved in the whole cross-section of the girder ($M = 75.0$ kNm)

4. CONCLUSIONS

In this paper, steel-timber composite beams with LVL slabs were analysed. Engineering wood products, e.g., laminated veneer lumber, have reintroduced wood as a viable material for complex structures. It is possible to replace slabs made of non-renewable concrete with slabs made of renewable and eco-friendly LVL. The significant advantages of using LVL in conjunction with steel were demonstrated. Composite action provided for increased bending resistance. The design plastic moment resistance of the beam section increased 6.1 times after the steel girder was connected to the LVL slab. In the case of the steel-timber composite beam with the slab narrower than the effective width, the plastic moment resistance of the beam section increased 2.4 times. The increase in the LVL slab thickness, the cross-section of the steel girder, and the yield strength of the steel provided for the increase in the bending resistance. The elastic and plastic resistance to bending estimated analytically and obtained in a numerical simulation were compared, yielding similar results. However, only the beams with full shear interaction and full shear connection were analysed and only theoretical and numerical analyses were conducted. Connections in steel-timber composite beams are flexible and the impact of slipping on the stiffness and the load bearing capacity of steel-timber composite beams should be investigated in future studies. Laboratory tests are recommended, and their results should be weighed against the results of theoretical and numerical analyses. Last but not the least, the effects of the degree of shear connection should also be investigated.

FUNDING

This research was funded by the Polish Ministry of Science and Higher Education under grant 0412/SBAD/0070.

REFERENCES

1. Nawrot, J 2023. *Perspektywy rozwoju rozwiązań materiałowo-konstrukcyjnych belek zespolonych w świetle najnowszych badań*. XIII Konferencja Naukowa Konstrukcje Zespolone 2023, Zielona Góra, 29-30 czerwca 2023, Poland, 31–32. (In Polish)
2. Puettmann, M, Pierobon, F, Ganguly, I, Gu, H, Chen, C, Liang, S, Jones, S, Maples, I and Wishnie, M 2021. Comparative LCAs of Conventional and Mass Timber Buildings in Regions with Potential for Mass Timber Penetration. *Sustainability* **13**, 13987. <https://doi.org/10.3390/su132413987>.
3. Ramage, MH, Burrige, H, Busse-Wicher, M, Fereday, G, Reynolds, T, Shah, DU, Wu, G, Yu, L, Fleming, P, Densley-Tingley, D, Allwood, J, Dupree, P, Linden, PF and Scherman, O 2017. The wood from the trees: The use of timber in construction. *Renewable and Sustainable Energy Reviews* **68**, Part 1, 333-359. <https://doi.org/10.1016/j.rser.2016.09.107>.

4. Yadav, R and Kumar, J 2022. Engineered Wood Products as a Sustainable Construction Material: A Review. In: Gong, M (ed) *Engineered Wood Products for Construction*, IntechOpen. <https://doi.org/10.5772/intechopen.99597>.
5. Chybiński, M and Polus, Ł 2021. Experimental and numerical investigations of laminated veneer lumber panels. *Archives of Civil Engineering* **67**, 351-372. <https://doi.org/10.24425/ace.2021.138060>.
6. Komorowski, M 2017. Podręcznik Projektowania i Budowania w Systemie STEICO. Podstawy. Fizyka Budowli. Zalecenia Wykonawcze. Warsaw: Forestor Communication. (In Polish)
7. Li, M, He, M and Li, Z. 2023. Size effects on the bending strength of Chinese larch pine laminated veneer lumber. *European Journal of Wood and Wood Products* **81**, 1211-1222. <https://doi.org/10.1007/s00107-023-01933-8>.
8. Bakalarz, MM and Kossakowski, PG 2022. Strengthening of Full-Scale Laminated Veneer Lumber Beams with CFRP Sheets. *Materials* **15**, 6526. <https://doi.org/10.3390/ma15196526>.
9. Chybiński, M, Polus, Ł and Szumkuć, W 2021. Zastosowanie drewna klejonego warstwowo z fornirów LVL w budownictwie. *Przegląd Budowlany* **5-6**, 44-50. (In Polish)
10. Dobes, P, Lokaj, A, Ponistova, L and Papesch, R 2019. Bending stiffness of selected types of glued I-beams made of wood-based materials. *ARP Journal of Engineering and Applied Sciences* 2019, **14**(7), 1357-1361.
11. Rodacki, K 2017. The load-bearing capacity of timber-glass composite I-beams made with polyurethane adhesives. *Civil and Environmental Engineering Reports* **27**(4), 105-120. <https://doi.org/10.1515/ceer-2017-0054>.
12. Kozłowski, M and Hulimka J. 2014. Load-bearing capacity of hybrid timber-glass beams. *Architecture, Civil Engineering, Environment* **7**(2), 61-71.
13. Ganowicz, R and Plenzler, R. 1978. *Zbrojone stalą belki drewniane – badania i realizacja obiektu prototypowego*. Sympozjum nt. „Badania nad zastosowaniem drewna i materiałów drewnopochodnych we współczesnych konstrukcjach budowlanych”, Szczecin, Poland. (In Polish)
14. Rajczyk, M and Stachecki, B. 2011. Przegląd rozwiązań konstrukcyjnych wzmacniania belek z drewna klejonego zbrojeniem w postaci prętów. *Zeszyty Naukowe Politechniki Częstochowskiej, Budownictwo*, z. **17**(167), 186-195. (In Polish)
15. Jasińko, J. 1988. Opracowanie metod wzmacniania konstrukcji drewnianych przy zastosowaniu żywic syntetycznych, Etap I. Raport Instytutu Budownictwa Politechniki Wrocławskiej. Wrocław, Poland. (In Polish)
16. Jasińko, J. 1989. Opracowanie metod wzmacniania konstrukcji drewnianych przy zastosowaniu żywic syntetycznych, Etap II. Raport Instytutu Budownictwa Politechniki Wrocławskiej, Wrocław, Poland. (In Polish)
17. Jasińko, J. 2003. Połączenia klejowe i inżynierskie w naprawie, konserwacji i wzmacnianiu zabytkowych konstrukcji drewnianych. Wrocław: Dolnośląskie Wydawnictwo Edukacyjne. (In Polish)
18. Nowak, T. 2007. Analiza pracy statycznej zginanych belek drewnianych wzmacnianych przy użyciu CFRP. PhD Thesis. Wrocław University of Technology. (In Polish)
19. Rapp, P. 2015. Metodyka i przykłady rewaloryzacji konstrukcji drewnianych w obiektach zabytkowych. *Wiadomości Konserwatorskie* **43**, 92-108. <https://doi.org/10.17425/WK43WOODENSTRUCT>.
20. Abramowicz, M, Berczyński, S and Wróblewski, T. 2020. Modelling and parameter identification of steel–concrete composite beams in 3D rigid finite element method. *Archives of Civil and Mechanical Engineering* **20**, 103. <https://doi.org/10.1007/s43452-020-00100-7>.

21. Grzeszykowski, B and Szmigiera, E. 2019. Nonlinear longitudinal shear distribution in steel-concrete composite beams. *Archives of Civil Engineering* **65**(1), 65-82, <https://doi.org/10.2478/ace-2019-0005>.
22. Aspila, A, Heinisuo, M, Mela, K, Malaska, M and Pajunen, S. 2022. Elastic design of steel-timber composite beams. *Wood Material Science & Engineering* **17**(4), 243-252. <https://doi.org/10.1080/17480272.2022.2093128>.
23. Chybiński, M, Polus, Ł, Szwabiński, W and Niewiem, P. 2019. FE analysis of steel-timber composite beams. *AIP Conference Proceedings* **2078**(1), 020061. <https://doi.org/10.1063/1.5092064>.
24. Lacki, P, Derlatka, A, Kasza, P and Gao, S. Numerical study of steel–concrete composite beam with composite dowels connectors. *Computers & Structures* **255**, 106618. <https://doi.org/10.1016/j.compstruc.2021.106618>.
25. Lacki, P, Nawrot, J, Derlatka, A and Winowiecka, J. 2019. Numerical and experimental tests of steel-concrete composite beam with the connector made of top-hat profile. *Composite Structures* **211**, 244-253. <https://doi.org/10.1016/j.compstruct.2018.12.035>.
26. Tharmabala, T and Bakht, B 1984. *Steel-wood composite bridge*. 12th IABSE Congress, Vancouver, BC, Canada, 3-7 September, 1984, <https://doi.org/10.5169/seals-12263>.
27. Bakht, B and Krisciunas, R 1997. Testing a Prototype Steel-Wood Composite Bridge. *Structural Engineering International* **7**(1), 35-41. <https://doi.org/10.2749/101686697780495391>.
28. Chiniforush, AA, Akbarnezhad, A, Valipour, H and Malekmohammadi, S 2019. Moisture and temperature induced swelling/shrinkage of softwood and hardwood glulam and LVL: An experimental study. *Construction and Building Materials* **207**, 70-83. <https://doi.org/10.1016/j.conbuildmat.2019.02.114>.
29. EN 1993-1-1; Eurocode 3: Design of steel structures - Part 1-1: General rules and rules for buildings, European Committee for Standardization: Brussels, Belgium, 2005.
30. Mróz, K, Hager, I and Korniejenko, K 2016. Material solutions for passive fire protection of buildings and structures and their performances testing. *Procedia Engineering* **151**, 284-291. <https://doi.org/10.1016/j.proeng.2016.07.388>.
31. Riola-Parada, F 2016. Timber-steel hybrid beams for multi-storey buildings. Ph.D. Thesis, TU Wien.
32. Chybiński, M and Polus, Ł 2018. Bending resistance of metal-concrete composite beams in a natural fire. *Civil and Environmental Engineering Reports* **4**(28), 149-162. <https://doi.org/10.2478/ceer-2018-0058>.
33. Barber, D, Blount, D, Hand, JJ, Roelofs, M, Wingo, L, Woodson, J and Yang, F. 2022. Design Guide 37: Hybrid Steel Frames with Wood Floors. American Institute of Steel Construction.
34. Chybiński, M and Polus, Ł 2019. Theoretical, experimental and numerical study of aluminium-timber composite beams with screwed connections. *Construction and Building Materials* **226**, 317-330. <https://doi.org/10.1016/j.conbuildmat.2019.07.101>.
35. Chybiński, M, Polus, Ł and Szumigala, M 2022. Aluminium members in composite structures – a review. *Archives of Civil Engineering* **4**, 253-274. <https://doi.org/10.24425/ace.2022.143037>.
36. Gardner, L 2005. The use of stainless steel in structures. *Progress in Structural Engineering and Materials* **7**(2), 45-55. <https://doi.org/10.1002/pse.190>.
37. Gardner, L and Baddoo, NR 2006. Fire testing and design of stainless steel structures. *Journal of Constructional Steel Research* **62**(6), 532-543, <https://doi.org/10.1016/j.jcsr.2005.09.009>.
38. Gardner, L 2007. Stainless steel structures in fire. *Proceedings of the Institution of Civil Engineers - Structures and Buildings* **160**(3), 129-138. <https://doi.org/10.1680/stbu.2007.160.3.129>.

39. Kyvelou, P, Gardner, L and Nethercot, DA 2017. Design of Composite Cold-Formed Steel Flooring Systems. *Structures* **12**, 242-252, <https://doi.org/10.1016/j.istruc.2017.09.006>.
40. Stiemer, S, Tefamariam, S, Karacabeyli, E and Popovski, M 2012. Development of steel-wood hybrid systems for buildings under dynamic loads. Behaviour of Steel Structures in Seismic Areas STESSA 2012, January 9 – 11, Santiago, Chile.
41. Wang, X, Su, P, Liu, J, Chen, Z and Khan, K 2022. Seismic performance of light steel-natural timber composite beam-column joint in low-rise buildings. *Engineering Structures* **256**, 113969. <https://doi.org/10.1016/j.engstruct.2022.113969>.
42. Kyvelou, P, Gardner, L and Nethercot DA 2018. Finite element modelling of composite cold-formed steel flooring systems. *Engineering Structures* **158**, 28-42, <https://doi.org/10.1016/j.engstruct.2017.12.024>.
43. Hassanieh, A, Valipour, HR and Bradford, MA 2016. Experimental and numerical study of steel-timber composite (STC) beams. *Journal of Constructional Steel Research* **122**, 367-378, <https://doi.org/10.1016/j.jcsr.2016.04.005>.
44. Liu, R, Liu, J, Wu, Z, Chen, L and Wang, J 2022. A Study on the Influence of Bolt Arrangement Parameters on the Bending Behavior of Timber–Steel Composite (TSC) Beams. *Buildings* **12**(11), 2013, <https://doi.org/10.3390/buildings12112013>.
45. Szweczak, I, Rzeszut, K and Rozylo, P 2021. Structural behaviour of steel cold-formed sigma beams strengthened with bonded steel tapes. *Thin-Walled Structures* **159**, 107295. <https://doi.org/10.1016/j.tws.2020.107295>.
46. Chybiński, M and Garstecki, A 2017. Diagonal versus orthogonal ribs in stability of steel I beams. *Procedia Engineering* **172**, 172-177. <https://doi.org/10.1016/j.proeng.2017.02.046>.
47. Derlatka, A. 2023. *Analiza kompozytowej belki stalowo-OSB*. XIII Konferencja Naukowa Konstrukcje Zespólone 2023, Zielona Góra, 29-30 czerwca 2023, Poland, 59-60. (In Polish)
48. Awaludin, A, Rachmawati, K, Aryati, M and Danastri, AD 2015. Development of Cold Formed Steel – Timber Composite for Roof Structures: Compression Members. *Procedia Engineering* **125**, 850-856, <https://doi.org/10.1016/j.proeng.2015.11.052>.
49. Vella, N, Kyvelou, P, Buhagiar, S and Gardner, L 2023. Innovative shear connectors for composite cold-formed steel-timber structures: An experimental investigation. *Engineering Structures* **287**, 116120. <https://doi.org/10.1016/j.engstruct.2023.116120>.
50. Hassanieh, A, Valipour, HR and Bradford, MA 2016. Experimental and analytical behaviour of steel-timber composite connections. *Construction and Building Materials* **118**, 63-75. <https://doi.org/10.1016/j.conbuildmat.2016.05.052>.
51. Hassanieh, A, Valipour, HR and Bradford, MA 2016. Load-slip behaviour of steel-cross laminated timber (CLT) composite connections, *Journal of Constructional Steel Research* **122**, 110-121, <https://doi.org/10.1016/j.jcsr.2016.03.008>.
52. Ataei, A, Chiniforush, AA, Bradford, MA, Valipour, HR and Ngo, TD 2022. Behaviour of embedded bolted shear connectors in steel-timber composite beams subjected to cyclic loading. *Journal of Building Engineering* **54**, 104581. <https://doi.org/10.1016/j.jobe.2022.104581>.
53. Zhao, Y, Yuan, Y, Wang, C-L and Meng, S 2023. Experimental and finite element analysis of flexural performance of steel-timber composite beams connected by hybrid-anchored screws. *Engineering Structures* **292**, 116503. <https://doi.org/10.1016/j.engstruct.2023.116503>.
54. Zhou, Y, Zhao, Y, Wang, C-L, Zhou, Y and Zheng, J 2022. Experimental study of the shear performance of H-shaped aluminum-timber composite connections. *Construction and Building Materials* **334**, 127421. <https://doi.org/10.1016/j.conbuildmat.2022.127421>.

55. Chybiński, M and Polus, Ł 2022 Mechanical Behaviour of Aluminium-Timber Composite Connections with Screws and Toothed Plates. *Materials* **15**, 68. <https://doi.org/10.3390/ma15010068>.
56. Romero, A, Yang, J, Hanus, F and Odenbreit, C 2022. Numerical Investigation of Steel-LVL Timber Composite Beams. *ce/papers* **5**, 21-30. <https://doi.org/10.1002/cepa.1694>.
57. Loss, C and Davison, B. 2017. Innovative composite steel-timber floors with prefabricated modular components. *Engineering Structures* **132**, 695-713. <https://doi.org/10.1016/j.engstruct.2016.11.062>.
58. Bradford, MA, Hassanieh, A, Valipour, HR and Foster, SJ 2017. Sustainable Steel-timber Joints for Framed Structures. *Procedia Engineering* **172**, 2-12. <https://doi.org/10.1016/j.proeng.2017.02.011>.
59. Abed, J, Rayburg, S, Rodwell, J and Neave, M 2022. A Review of the Performance and Benefits of Mass Timber as an Alternative to Concrete and Steel for Improving the Sustainability of Structures. *Sustainability* **14**, 5570. <https://doi.org/10.3390/su14095570>.
60. EN 1994-1-1; Eurocode 4, Design of Composite Steel and Concrete Structures—Part 1-1: General Rules and Rules for Buildings. European Committee for Standardization: Brussels, Belgium, 2004.
61. Strzelecka, J 2023. An analysis of the load bearing capacity and stiffness of steel – timber composite beams with steel I-beams and laminated veneer lumber (LVL) slabs. Master Thesis. Poznan University of Technology. (In Polish)
62. Kozłowski, A 2017. Podręcznik projektowania konstrukcji ze stali nierdzewnych. Rzeszów: Oficyna Wydawnicza Politechniki Rzeszowskiej. (In Polish)
63. Chybiński, M and Polus, Ł 2021. Experimental and numerical investigations of aluminium-timber composite beams with bolted connections. *Structures* **34**, 1942-1960. <https://doi.org/10.1016/j.istruc.2021.08.111>.
64. Chybiński, M and Polus, Ł 2023. Structural Behaviour of Aluminium–Timber Composite Beams with Partial Shear Connections. *Applied Sciences* **13**, 1603. <https://doi.org/10.3390/app13031603>.
65. Szewczyk, P and Szumigała, M 2021. Optimal Design of Steel–Concrete Composite Beams Strengthened under Load. *Materials* **14**, 4715. <https://doi.org/10.3390/ma14164715>.
66. Pełka-Sawenko, A, Wróblewski, T and Szumigała, M 2016. Validation of Computational Models of Steel-Concrete Composite Beams. *Engineering Transactions* **64**(1), 53-67.
67. Alawdin, P and Urbańska, K 2011. Limit analysis of steel-concrete composite structures with slip. *Civil and Environmental Engineering Reports* **7**, 19-34.
68. Dorn, M, Habrová, K, Koubek, R and Serrano, E 2020. Determination of coefficients of friction for laminated veneer lumber on steel under high pressure loads. *Friction*. <https://doi.org/10.1007/s40544-020-0377-0>.
69. Abaqus 6.13 Documentation, Abaqus Analysis Users Guide, Abaqus Theory Guide.
70. Rozyło, P 2021. Failure analysis of thin-walled composite structures using independent advanced damage models. *Composite Structures* **262**, 113598. <https://doi.org/10.1016/j.compstruct.2021.113598>.